

Preparation of polymer coated superparamagnetic Iron Oxide (Fe_3O_4) nanoparticles for biomedical application

I. Karimzadeh¹; M. Aghazadeh^{2*}; S. Shirvani-Arani³

¹ Shefa Neuroscience Research Center, Khatam ol Anbia Specialty and Subspecialty Hospital, Tehran, Iran

² NFCRI, Nuclear Science and Technology Research Institute (NSTRI), P.O. Box 14395-834, Tehran, Iran

³ NFCRI, Nuclear Research Institute, Tehran, Iran

Received: 14 December 2015; Accepted: 17 February 2016

ABSTRACT: Biomedical applications of superparamagnetic iron oxide nanoparticles (SPIONs) requiring precise control over their physical and magnetic properties, and proper surface treatment. Here we report a practical and effective electrochemical strategy for preparation of the polymer coated SPIONs. In this strategy, *in situ* polymer coating on the surface of SPIONs was achieved through electrodeposition process. The evaluation by XRD analysis confirmed that the electrodeposited sample has pure phase of iron oxide i.e. magnetite (Fe_3O_4). The PEG/PVC coating of SPIONs was confirmed by FTIR, DLS and DSC-TG analyses. The FE-SEM observation and DLS analysis revealed that the prepared polymer coated SPIONs have proper dispersion and nanosize about 20 nm. The magnetic measurement by VSM revealed that the prepared SPIONs exhibit excellent superparamagnetic behavior, showing high magnetization value ($M_s = 32 \text{ emu/g}$), and negligible coercivity ($C_e = 0.42 \text{ emu/g}$) and remanence ($M_r = 1.1 \text{ Oe}$) values. Based on the obtained results, it was concluded that this electrochemical strategy is facile and effective method for preparation of polymer coated Fe_3O_4 nanoparticles for biomedical applications.

Keywords: Biomedical Application; Electrochemical Synthesis; Fe_3O_4 : Nanoparticles; Polymer coating

INTRODUCTION

In the recent years, the synthesis of superparamagnetic iron oxide nanoparticles (SPIONs) has been intensively developed not only for its fundamental scientific interest but also for many biomedical and bioengineering applications including cell targeting and separation, MR imaging, cancer treatment, hyperthermia, gene and drug delivery (Chomoucka, *et al.*, 2010, Sharma, *et al.*, 2014, Gupta and Wells, 2004, Gupta and Gupta,

2005). These unique special applications of SPIONs are strongly dedicated by their size, surface and magnetic behavior (Reddy, *et al.*, 2012, Somaskandan, *et al.*, 2008, Laurent, *et al.*, 2008). All of these biomedical applications require that the nanoparticles have high magnetization values, a size smaller than 100 nm, and a narrow particle size distribution. So, the control of the monodisperse size is very important because the properties of the nanocrystals depend upon the dimen-

* Corresponding Author - e-mail: maghazadeh@aeoi.org.ir

sion of the nanoparticles. Also, appropriate surface chemistry of SPIONs is essential factor for numerous in vivo applications which has to be nontoxic and biocompatible and must also allow for a targetable delivery with particle localization in a specific area (Laurent, *et al.*, 2008).

Until now, various synthesis routes have been developed for the preparation of monodispersed SPIONs in the solution phase (Farahmandjou, *et al.*, 2014, Sharafi and Seyedadjadi, 2013, Wang, *et al.*, 2014, Hufschmid, *et al.*, 2015, Sharma and Jeevanandam, 2013, Mandel, *et al.*, 2015, Turcheniuk, *et al.*, 2013, Lu, *et al.*, 2010). For example, co-precipitation of Fe^{3+} and Fe^{2+} salts is a classical method employed to prepare water-soluble and biocompatible iron oxide NPs (Farahmandjou, *et al.*, 2014, Sharafi and Seyedadjadi, 2013, Wang, *et al.*, 2014, Hufschmid, *et al.*, 2015). Fe_3O_4 NPs are also prepared by aging a stoichiometric mixture of ferrous and ferric hydroxides in aqueous media or partially oxidized ferrous hydroxide suspensions with oxidizing agents. The size and morphology of the NPs can be controlled by adjusting the pH, reaction temperature, precursors, and the $\text{Fe}^{2+}/\text{Fe}^{3+}$ concentration ratio. However, this method leads to reduced control of particle shape, broad distributions of sizes and aggregation of particles. High temperature decomposition is recently used to obtain SPIONs with controlled size and morphology via high temperature decomposition of iron precursors in the presence of hot organic surfactants (Hufschmid, *et al.*, 2015, Sharma and Jeevanandam, 2013, Mandel, *et al.*, 2015, Turcheniuk, *et al.*, 2013, Lu, *et al.*, 2010). The size and shape of iron oxide NPs could be controlled by adjusting the reaction temperature and the molar ratio of precursor to stabilizer. This approach is a common method to synthesize various iron oxides, including Fe_3O_4 (magnetite), $\gamma\text{-Fe}_2\text{O}_3$ (maghemite) and $\alpha\text{-Fe}_2\text{O}_3$ (hematite) NPs (Tsouris, *et al.*, 2001). However, this method usually requires a complicated process and high temperature. Electrochemical synthesis i.e. electrodeposition is a promising alternative technique for fabrication of SPIONs, because of its facility and ability to control purity, crystallinity and size of deposited Fe_3O_4 by manipulating the current or the potential applied to the system (Tsouris, *et al.*, 2001, Cabrera, *et al.*, 2008). Until now, both anodic and cathodic elec-

trodeposition regimes have been used for preparation of SPIONs (Tsouris, *et al.*, 2001, Cabrera, *et al.*, 2008, Rodriguez-Lopez, *et al.*, 2012, Fajaroh, *et al.*, 2012, Pascal, *et al.*, 1999, Starowicz, *et al.*, 2011, Salamun, *et al.*, 2011, Ying, *et al.*, 2002, Carlier, *et al.*, 2005, Aghazadeh, *et al.*, 2016, Aghazadeh, *et al.*, 2016, Tizfahm, *et al.*, 2016). In the case of anodic electro-synthesis of SPIONs, many reports are available in literature (Tsouris, *et al.*, 2001, Cabrera, *et al.*, 2008, Rodriguez-Lopez, *et al.*, 2012, Fajaroh, *et al.*, 2012, Pascal, *et al.*, 1999, Starowicz, *et al.*, 2011, Salamun, *et al.*, 2011, Ying, *et al.*, 2002, Carlier, *et al.*, 2005). For example, Cabrera et al. (Cabrera, *et al.*, 2008) prepared Fe_3O_4 NPs with sizes between 20 and 30 nm by Fe electrooxidation in the presence of an amine surfactant. They observed that the increase in current density or potential promotes higher size homogeneity of the nanoparticles, but metallic Fe is formed as an impurity. Furthermore, they noted that the distance between anode and cathode (<5cm) is a key parameter to obtain Fe_3O_4 by electrooxidation. Rodriguez-Lopez et al. (Rodriguez-Lopez, *et al.*, 2012) prepared Fe_3O_4 and $\gamma\text{-Fe}_2\text{O}_3$ NPs with controlled size distribution by applying a dissymmetric pattern of potential pulses to iron-based electrodes in aqueous media. They found that Fe_3O_4 nanoparticles without any impurities (i.e. metallic iron particles) can be formed at the conditions of large anodic potentials and longest time. The prepared NPs in that work (Rodriguez-Lopez, *et al.*, 2012) had quasi spherical shape and the size ranged from 10 to 50 nm. Fajaroh et al. (Fajaroh, *et al.*, 2012) reported magnetite nanoparticles prepared by surfactant-free anodic deposition. They found that OH⁻ ions play an important role in the formation of Fe_3O_4 NPs, and particle size can be also controlled by adjusting the current density and the distance between electrodes. Pascal et al. synthesized amorphous $\gamma\text{-Fe}_2\text{O}_3$ NPs by anodic dissolution of a sacrificial Fe anode, followed by chemical reaction in an organic medium (Pascal, *et al.*, 1999). Starowicz reported $\gamma\text{-Fe}_2\text{O}_3$ preparation by anodic polarization of iron from the solution of 0.1 M LiCl in mixed water-ethanol electrolyte, and found that the size of the obtained nanoparticles can be controlled through regulating water content (Starowicz, *et al.*, 2011). In fact, they found that the smaller Fe_3O_4 particles are formed in mixed ethanol/water elec-

troytes due to reduction of the anodic reaction rate. From reviewing these works, it is revealed that anodic deposition has some requisites of applying high voltage (40-62V) (Starowicz, *et al.*, 2011, Salamun, *et al.*, 2011), distance between electrodes (<5cm) (Fajarooh, *et al.*, 2012, Pascal, *et al.*, 1999, Starowicz, *et al.*, 2011, Salamun, *et al.*, 2011, Ying, *et al.*, 2002, Carlier, *et al.*, 2005), supporting electrolyte and/or surfactant (Cabrera, *et al.*, 2008, Fajarooh, *et al.*, 2012), and the product are mixed phases in some cases (Cabrera, *et al.*, 2008, Pascal, *et al.*, 1999, Starowicz, *et al.*, 2011, Salamun, *et al.*, 2011). It was reported that cathodic deposition can be considered as an effective procedure for the synthesis of metal oxides (Aghazadeh, *et al.*, 2016, Aghazadeh, *et al.*, 2016, Tizfahm, *et al.*, 2016, Barani, *et al.*, 2014, Aghazadeh, *et al.*, 2012, Aghazadeh, *et al.*, 2013), and this method has not practical crises and no need for surfactant or supporting electrolyte and seems that can acquit suffers of anodic deposition disadvantages. However, there are only a few reports on the cathodic deposition of Fe_3O_4 NPs via base electrogeneration in literature (Park *et al.*, 2008, Marques *et al.*, 2008, Ibrahim *et al.*, 2009). Cathodic deposition of SPIONs in mixed water-ethanol solutions has been carried out by Verelst group for the first time in 2008 (Marques *et al.*, 2008). They proposed a mechanism pathway based on the $\text{Fe}(\text{OH})_3$ precipitation followed by its reduction to Fe_3O_4 (Ibrahim *et al.*, 2009). However, preparation of SPIONs through cathodic deposition route can be regarded as an interesting and yet unexplored area of research.

Here, we applied the cathodic electrodeposition for preparation of polymer coated SPIONs with desired size and dispersion from aqueous electrolyte. The polyethylene glycol (PEG) and polyvinyl alcohol (PVC) were used as coatings for SPIONs during the electrochemical synthesis. Notably, this one-step electrochemical preparation of polymer coated SPIONs has not been reported until now. The purity, well-dispersion, nanosize and superparamagnetic property of the prepared SPIONs were confirmed via XRD, SEM, VSM and IR techniques. The polymer coat of SPIONs was also confirmed via FTIR, TG and DLS analyses. In spite of the most used chemical routes which require long time (8-12h) and high temperature (40-60°C) for coating process, our developed method

is in situ, simple, one-pot and time conserving.

EXPERIMENTAL

Sample preparation

All chemicals were reagent-grade purity and obtained from commercial sources (Aldrich and Alfa Aesar) and used as received. Deposition experiments were conducted in the galvanostatic regime using a two-electrode system. The electrochemical cell included a cathodic stainless-steel cathode and graphite anode. Prior to each deposition, the steel substrates were galvanostatically electropolished at a current density of 0.5 A cm^{-2} for 5 min in a bath (70°C) containing 50 vol% phosphoric acid, 25 vol% sulfuric acid and balanced deionized water. A solution of 0.005 M $[\text{FeCl}_2/\text{Fe}(\text{NO}_3)_3]$ with molar ratio of 1:2 in addition to 1 g/L [PEG+PVC] was used as deposition bath composition. The Fe_3O_4 nanoparticles were electrodeposited in the presence of PEG and PVC polymers with applying the current density of 1 A/cm^2 for 30 min. The deposition experiments were performed using an electrochemical workstation system (Potentiostat/Galvanostat, Model: NCF-PGS 2012, Iran). After the deposition, the steel substrates were rinsed with distilled water several times and dried at 50°C for 5h. Finally the deposits were scraped from the substrates and evaluated by further analyses.

Sample characterization

The crystal structure of SPIONs was determined by powder X-ray diffraction (XRD, a Phillips PW-1800 diffractometer with Co K α radiation ($\lambda = 1.789 \text{ \AA}$)). FTIR spectra were obtained using a Bruker Vector 22 Fourier transformed infrared spectrometer. Each FTIR spectrum was collected after 20 scans at a resolution of 4 cm^{-1} from 400 to 4000 cm^{-1} . The morphology of the samples was studied using a scanning electron microscope (SEM, LEO 1455 VP, Oxford, UK, operating voltage 30 kV) by mounting a small amount of the prepared powders on a conducting carbon tape and sputter coating with Pt to improve the conductivity. Thermal behavior analysis were carried out in N_2 between room temperature and 400°C at a heating rate of 5°C min^{-1} using a thermoanalyzer (STA-1500).

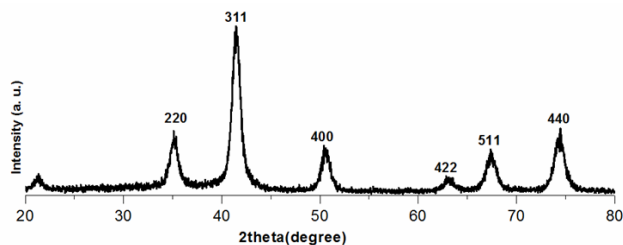


Fig. 1: XRD pattern of the prepared PEG/PVC coated SPI-ONs.

Hydrodynamic diameter and zeta potential of the prepared nanoparticles was determined by dynamic light scattering (DLS, 4700 Malvern Instruments, UK) at 632 nm wavelength laser and a scattering angle of 90° in aqueous solution as electrolyte. Vibrating sample magnetometer (VSM) (Model: Lake shore 7400, United States) was employed to study the hysteresis loops and the magnetic properties of the magnetite nanoparticles at room temperature from -20000 to 20000 Oe.

RESULTS AND DISCUSSION

Fig. 1 indicates the XRD pattern of the prepared sample. All diffraction peaks in this pattern can be easily indexed to the magnetite reflections (JCPDS 19-629 reference card, lattice parameter $a = 0.83980$ nm). No peak related to the any impurity was observed. The average crystallite size (D) was calculated from the diffraction line-width of XRD patterns, based on Scherrer's relation ($D = 0.9\lambda/\beta\cos\theta$), where, β is the full width at half maxima (FWHM) of the (311) peak. The size of prepared Fe_3O_4 NPs was obtained to be 14.1 nm.

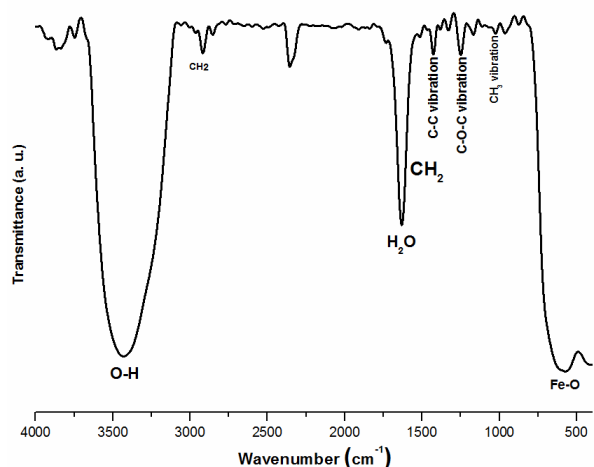


Fig. 2: IR spectrum of the prepared PEG/ PVC coated SPI-ONs.

The presence of PEG/PVC coat on the SPI-ONs surface was investigated by FTIR spectroscopy. Fig. 2 exhibits the IR spectra of the prepared nanoparticles. The band at 586 cm^{-1} is related to the stretching mode of Fe-O in Fe_3O_4 (Cabrera, *et al.*, 2008, Rodriguez-Lopez, *et al.*, 2012, Fajaroh, *et al.*, 2012), indicating the magnetite phase of the prepared sample. The absorption bands at 3465 and 1632 cm^{-1} are related to O-H stretching and deformation vibrations, respectively. These bands indicated the existence of hydroxyl groups attached on the surface of Fe_3O_4 nanoparticles (Carlier, *et al.*, 2005).

The following bands confirmed the polymer coat on the surface of prepared Fe_3O_4 NPs: (i) The bonds at 1172 cm^{-1} and 1335 cm^{-1} are due to the stretch and vibration of C-C bands (antisymmetric stretch), respectively (Kim, *et al.*, 2010, Hu, *et al.*, 2008), (ii) The peaks at about 1252 cm^{-1} and 1430 cm^{-1} which

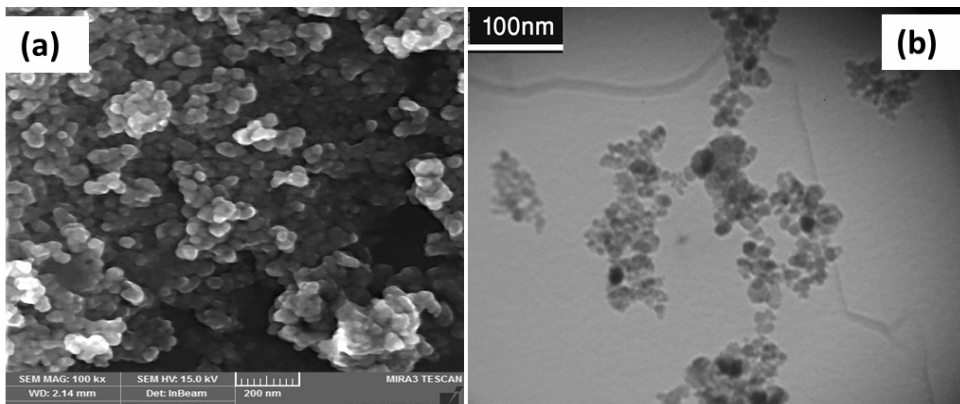


Fig. 3: (a) FE-SEM and (b) TEM images of the prepared PEG/ PVC coated SPI-ONs.

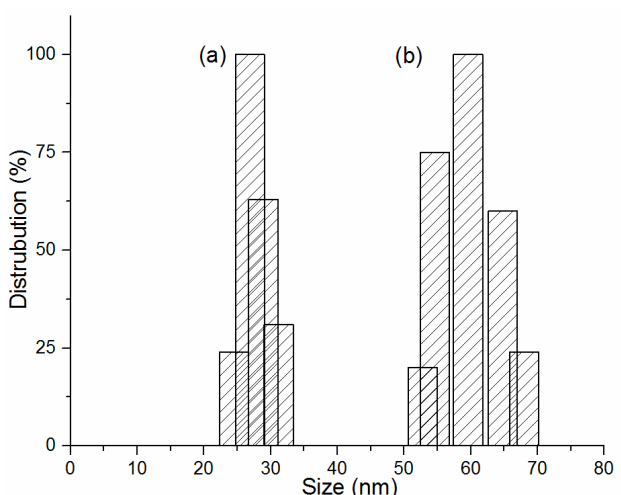


Fig. 4: Particle size distributions of (a) bare and (b) polymer coated SPIONs.

are assigned to the CH_2 vibrations (Kim, *et al.*, 2010), (iii) the bonds around 2905 cm^{-1} and 966 cm^{-1} indicating the bending vibrations of CH out-of-plane (Kim, *et al.*, 2010, Hu, *et al.*, 2008, Masoudi, *et al.*, 2012) and (iv) the peaks at 2926 cm^{-1} and 2877 cm^{-1} , which deal with to the asymmetric and symmetric stretching vibrations of C-H bonds, respectively (Masoudi, *et al.*, 2012). Also, the peaks located at 1122 cm^{-1} and 1381 cm^{-1} deal with to the C-O-C ether stretch and vibration bands (anti symmetric stretch) in PEG, respectively (Kim, *et al.*, 2010, Masoudi, *et al.*, 2012) and revealing the PEG coat on the SIONs surface. Furthermore, the peak at 625 cm^{-1} is related to the stretching vibration of C-Cl bond in PVC (Yao, *et al.*, 2015). So, IR analysis completely revealed the polymer coat i.e. PEG and PVC on the surface of the electrodeposited iron oxide nanoparticles.

Morphological characteristics of the prepared sample were determined by FE-SEM and TEM observations. The FE-SEM image of the prepared samples is shown in Fig. 3a. It can be seen that the electrodeposited sample has particle morphology and no obvious aggregation is observed. The mean diameter of Fe_3O_4 NPs was estimated to be $\sim 20\text{ nm}$ from measuring the diameter of several particles in FESEM image. For better observation of the prepared nanoparticles, the TEM images of the synthesized particles was provided, which is shown in Fig. 3b. The TEM observation is clearly shown that the prepared sample have particle morphology with proper dispersion and nanosize. The mean diameter of the prepared nanoparticles was

measured to be 15 nm , which are very close to the calculated size (i.e. 14.1 nm) from XRD pattern in Fig. 1.

The hydrodynamic diameter of the polymer coated nanoparticles was measured by using a DLS particle size analyzer. Fig. 4 illustrates the particle size distributions of the bare and polymer coated nanoparticles. For bare NPs (Fig. 4a), the mean hydrodynamic diameter was measured to be 26 nm . For the polymer coated NPs, this values is observed to be 59.6 , which are larger than those of bare NPs. These results clearly prove the polymer layer on the surface of magnetite nanoparticles.

The thermal properties of the prepared nanoparticles were studied by TGA and DSC and the results are shown in Fig. 5. For our samples, a multistep exothermic peak is observed in DSC curve between the temperatures of 100 and 600°C . Correspondingly, TG curve shows three major weight losses at these temperatures. At temperatures below 100°C , the observed weight losses is related to removal of the H_2O molecules connected on the surface of SPI-ONs as confirmed by FTIR analysis. In the literature, it was reported that PVC degradation is occurred at 200 - 250°C (Masoudi, *et al.*, 2012, Yao, *et al.*, 2015, Kok, *et al.*, 2008, Li, *et al.*, 2000, Santra, *et al.*, 2001). Therefore, the sharp change in DSC and TG curved at 225 - 250°C is due to the PVC decomposition. The mass loss during PVC degradation includes sequential loss of hydrogen chloride accompanied by the generation of polyene sequences (Kok, *et al.*, 2008, Li, *et al.*, 2000, Santra, *et al.*, 2001). Notably, it was reported

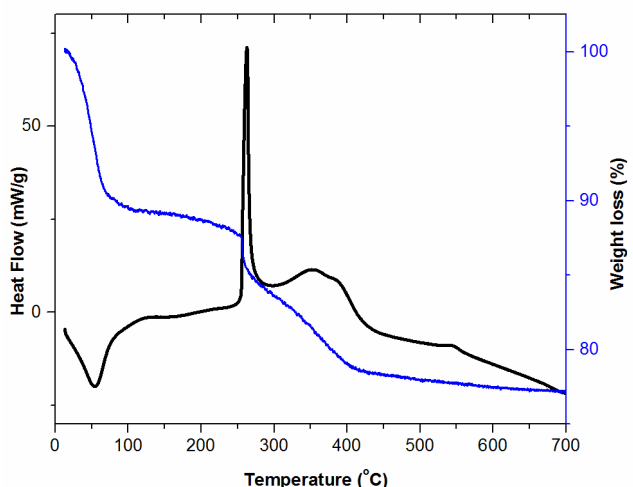


Fig. 5: DSC-TG curves for the prepared PEG/P PVC coated SPIONs.

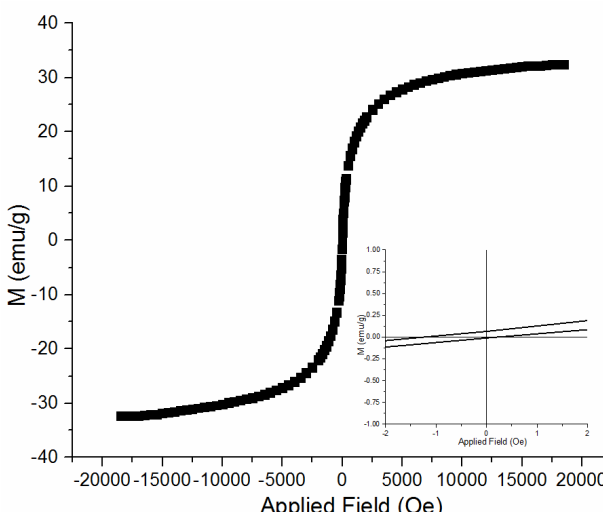


Fig. 6: VSM curve for the prepared PEG/ PVC coated SPIONs.

that the decomposition of pure PEG started at around 350°C and ended at 425°C (Junejo, *et al.*, 2013). In the literature, it was also observed that the decomposition of PEG coat of NPs is started around 177°C and ended at around 352°C (Junejo, *et al.*, 2013, Viali, *et al.*, 2013, Barrera, *et al.*, 2012, Mukhopadhyay, *et al.*, 2012). So, the weight loss observed at this temperature range is related to the PEG decomposition on the SPIONs surface. The TG curve exhibit the total weight losses of 23.44 %. This change in the profile of TG curve confirmed the attachment of PEG/PVC molecules onto the surface of SPIONs. After 550°C, there is practically no change in weight throughout the temperature range up to 700°C (Fig. 5) indicating the complete decomposition of polymer coat on the nanoparticles. These results confirmed the in situ coating of the Fe_3O_4 nanoparticles during their cathodic electrodeposition.

The magnetic properties of the prepared Fe_3O_4 nanoparticles were measured at room temperature using vibrating sample magnetometer, as shown in Fig. 6. It can be seen that the magnetization curve has s-shaped over the applied magnetic field and the samples exhibit typical superparamagnetic behavior, showing high M_s value and negligible C_e and M_r values. The Saturation Magnetization (M_s), Coercivity (C_e) and Remanence (M_r) values were calculated from the M-H curves to be 32 emu/g, 0.42 emu/g and 1.1 Oe, respectively. For clinical applications like an MRI contrast agent, it is critical that SPIONs retain

their magnetic properties after the modification treatments. Therefore, it can be stated that the prepared polymer coated SPIONs have proper characteristics for biomedical applications.

CONCLUSIONS

In summary, a practical and effective strategy for synthesizing polymer coated SPIONs is developed. In this strategy, magnetite nanoparticles were prepared via cathodic electrodeposition in aqueous medium and the surface coating was successfully performed during their electrochemical preparation. The synthesized PEG/PVC coated SPIONs were characterized by FTIR, DLS, TGA, FE-SEM and VSM. The results confirmed the proper size and distribution, polymer coat and magnetic properties of the prepared SPIONs for biomedical applications.

REFERENCES

- Aghazadeh, M.; Ghaemi, M.; Golikand, A.N.; Ahmadi, A., (2012). Porous network of Y_2O_3 nanorods prepared by electrogeneration of base in chloride medium. Mater. Lett., 65: 2545-2548.
- Aghazadeh, M.; Hosseinfard, M., (2013). Electrochemical preparation of ZrO_2 nanopowder: impact of the pulse current on the crystal structure, composition and morphology. Ceram. Int., 39: 4427-4435.
- Aghazadeh, M.; Ghannadi Maragheh, M.; Ganjali, M.R.; Norouzi, P.; Faribod, F., (2016). Electrochemical preparation of MnO_2 nanobelts through pulse base-electrogeneration and evaluation of their electrochemical performance. Appl. Surf. Sci., 364: 141-147.
- Aghazadeh, M.; Asadi, M.; Ghannadi Maragheh, M.; Ganjali, M.R.; Norouzi, P.; Faribod, F., (2016). Facile preparation of MnO_2 nanorods and evaluation of their supercapacitive characteristics. Appl. Surf. Sci., 364: 726-731.
- Barani, A.; Aghazadeh, M.; Ganjali, M.R.; Sabour, B.; Barmi, A.A.M.; Dalvand, S., (2014). Nanostructured nickel oxide ultrafine nanoparticles: Synthe-

- sis, characterization, and supercapacitive behavior. *Mater. Sci. Semiconduc. Process.*, 23: 85-92.
- Barrera, C.; Herrera, A.P.; Bezares, N.; Fachini, E.; Olayo-Valles, R.; Hinestroza, J.P.; Rinaldi C., (2012). Effect of poly (ethylene oxide)-silane graft molecular weight on the colloidal properties of iron oxide nanoparticles for biomedical applications. *J. Colloid Interf. Sci.*, 377: 40-50.
- Carlier, D.; Terrier, C.; Arm, C.; Anserment, J.P., (2005). Preparation and magnetic properties of Fe_3O_4 nanostructures grown by electrodeposition. *Electrochim. Solid-State Lett.*, 8: C43- C46.
- Cabrera, L.; Gutierrez, S.; Menendez, N.; Morales, M.P.; Herrasti, P., (2008). Magnetite nanoparticles: electrochemical synthesis and characterization. *Electrochim. Acta*, 53: 3436-3441.
- Chomoucka, J.; Drbohlavova, J.; Huska, D.; Adam, V.; Kizek, R.; Hubalek, J., (2010). Magnetic nanoparticles and targeted drug delivering. *Pharmacol. Res.*, 62: 144-149.
- Fajaroh, F.; Setyawan, H.; Widiyastuti, W.; Winardi, S., (2012). Synthesis of magnetite nanoparticles by surfactant-free electrochemical method in an aqueous system. *Adv. Powder. Technol.*, 23: 328-333.
- Farahmandjou, M.; Soflaee, F., (2014). Synthesis of Iron Oxide nanoparticles using borohydride reduction. *Int. J. Bio-Inorg. Hybr. Nanomater.*, 3: 203-206.
- Gupta, A.K.; Gupta, M., (2005). Synthesis and surface engineering of iron oxide nanoparticles for biomedical applications. *Biomater.*, 26: 3995-4021.
- Gupta, A.K.; Wells S., (2004). Surface-modified superparamagnetic nanoparticles for drug delivery: preparation, characterization, and cytotoxicity studies. *IEEE Trans. Nanobiosci.*, 3: 66-73.
- Hu, L.; Hach, D.; Chaumont, D.; Brachais, C.H.; Couvercelle, J.P., (2008). One step grafting of mono-methoxy poly(ethylene glycol) during synthesis of maghemite nanoparticles in aqueous medium. *Colloids Surf. A.*, 330: 1-7.
- Hufschmid, R.; Arami, H.; Matthew Ferguson, R.; Gonzales, M.; Teeman, E.; Brush, L.N.; Browning, N.D.; Krishnan, K.M., (2015). Synthesis of phase-pure and monodisperse iron oxide nanoparticles by thermal decomposition. *Nanoscale.*, 7: 11142-11154.
- Ibrahim, M.; Serrano, K.G.; Noea, L.; Garcia, C.; Verelst, M.; (2009). Electro-precipitation of magnetite nanoparticles: An electrochemical study. *Electrochim. Acta*, 55: 155-158.
- Junejo, Y.; Baykal, A.; Sozeri, H., (2013). Simple hydrothermal synthesis of Fe_3O_4 -PEG nanocomposite. *Eur. J. Chem.*, 11: 1527-1532.
- Kim, M.; Jung, J.; Lee, J.; Na, K.; Park, S.; Hyun, J., (2010). Amphiphilic comb like polymers enhance the colloidal stability of Fe_3O_4 nanoparticles. *Colloids Surf. B.*, 76: 236-240.
- Kok, M.; Demrelli, K.; Aydogdu, Y., (2008). Thermo-physical properties of blend of poly (vinyl chloride) with poly (isobornyl acrylate). *Int. J. Sci. Technol.*, 3: 37-42.
- Laurent, S.; Forge, D.; Port, M.; Roch, A., Robic, C.; Vander Elst, L.; Muller, R.N., (2008). Magnetic iron oxide nanoparticles: synthesis, stabilization, vectorization, physicochemical characterizations, and biological applications. *Chem. Rev.*, 108: 2064-2110.
- Li, B., (2000). A study of thermal degradation and decomposition of rigid poly(vinyl chloride) with metal oxides using thermogravimetry and cone calorimetry. *Polym. Degrad. Stabil.*, 68: 197-204.
- Lu, C.; Quan, Z.S.; Sur, J.C.; Kim, S.H.; Lee, C.H.; ChaiI, K.Y., (2010) One-pot fabrication of carboxyl-functionalized biocompatible magnetic nanocrystals for conjugation with targeting agents. *New J. Chem.*, 34, 2040-2046.
- Mandel, K.; Straber, M.; Granath, T.; Dembski, S.; Sextla, G., (2015). Surfactant free superparamagnetic iron oxide nanoparticles for stable ferrofluids in physiological solutions. *Chem. Commun.*, 51, 2863-2866.
- Marques, R.F.C.; Garcia, C.; Lecante, P.; Ribeiro, S.J.L.; Noe, L.; Silva, N.J.O.; Amaral, V.S.; Millan, A.; Verelst M., (2008). Electro-precipitation of Fe_3O_4 nanoparticles in ethanol. *J. Magn. Magn. Mater.*, 320: 2311-2315.
- Masoudi, A.; Madaah Hosseini, H.R.; Shokrgozar, M.A.; Ahmadi, R.; Oghabian, M.A., (2012). The effect of poly(ethylene glycol) coating on colloidal stability of superparamagnetic iron oxide nanoparticles as potential MRI contrast agent. *Int.*

- J. Pharmaceut., 433:129-141.
- Mukhopadhyay, A.; Joshi, N.; Chattopadhyay, K.; De, G., (2012). *Acs. Appl. Mater. Inter.*, 4: 142-149.
- Park, H.; Ayala, P.; Deshusses, M.A.; Mulchandani, A.; Choi, H.; Myung, N.V., (2008). Electrodeposition of maghemite (γ -Fe₂O₃) nanoparticles. *Chem. Engin. J.*, 139: 208-212.
- Pascal, C.; Pascal, J.L.; Favier, F., (1999). Electrochemical synthesis for the control of α -Fe₂O₃ nanoparticle size. morphology, microstructure, and magnetic behavior. *Chem. Mater.*, 11: 141-147.
- Reddy, L.H.; Arias, J.L.; Nicolas, J.; Couvreur, P., (2012). Magnetic nanoparticles: design and characterization, toxicity and biocompatibility, Pharmaceutical and biomedical applications. *Chem. Rev.*, 112: 5818-5878.
- Rodríguez-Lopez, A.; Paredes-Arroyo, A.; Mojica-Gómez, J.; Estrada-Arteaga, C.; Cruz-Rivera, J.J.; Elias Alfaro, C.G.; Antano-Lopez, R., (2012). Electrochemical synthesis of magnetite and maghemite nanoparticles using dissymmetric potential pulses. *J. Nanopart. Res.*, 14: 993-1001.
- Santra, S.; Tapec, R.; Theodoropoulou, N.; Dobson, J.; Hebard, A.; Tan, W., (2001). Synthesis and Characterization of Silica-Coated Iron Oxide Nanoparticles in Microemulsion: The Effect of Nonionic Surfactants. *Langmuir*, 17: 2900-2906.
- Salamun, N.; Ni, H.X.; Triwahyono, S.; Abdul Jalil, A.; Hakimah Karim, A., (2011). Synthesis and characterization of Fe₃O₄ nanoparticles by electrodeposition and reduction methods. *J. Fundamental Sci.*, 7: 89-92.
- Sharafi, A.; Seyedsadjadi, M., (2013). Surface-modified superparamagnetic nanoparticles Fe₃O₄@PEG for drug delivery pages. *Int. J. Bio-Inorg. Hybd. Nanomat.*, 3: 437-441.
- Sharma, P.; Rana, S.; Barick, K.C.; Kumar, C.; Salunkhe, H.G.; Hassan, P.A., (2014). Biocompatible phosphate anchored Fe₃O₄ nanocarriers for drug delivery and hyperthermia. *New J. Chem.*, 38: 5500-5508.
- Sharma, G.; Jeevanandam, P., (2013). Synthesis of self-assembled prismatic iron oxide nanoparticles by a novel thermal decomposition route. *RSC Adv.*, 3: 189-200.
- Somaskandan, K.; Veres, T.; Niewczas, M.; Simard, B., (2008). Surface protected and modified iron based core-shell nanoparticles for biological applications. *New J. Chem.*, 32: 201.
- Starowicz, M.; Starowicz, P.; Zukrowski, J.; Przewoznik, J.; Lemanski, A.; Kapusta, C.; Banas, J., (2011). Electrochemical synthesis of magnetic iron oxide nanoparticles with controlled size. *J. Nanopart. Res.*, 13: 7167-7176.
- Tizfahm, J.; Aghazadeh, M.; Ghannadi Maragheh, M.; Ganjali M.R.; Norouzi P.; Faridbod F., (2016). Electrochemical preparation and evaluation of the supercapacitive performance of MnO₂ nano-worms. *Mater. Lett.*, 167: 153-156.
- Tsouris, C.; DePaoli, D.W.; Shor, J.T., US, (2001). Method and apparatus to electrolytically produce high-purity magnetite particles. UT Battelle, LLC.
- Turcheniuk, K.; Tarasevych, A.V.; Kukhar, V.P.; Boukherroub, R.; Szunerits, S., (2013). Recent advances in surface chemistry strategies for the fabrication of functional iron oxide based magnetic nanoparticles. *Nanoscale*, 5: 10729- 10752.
- Viali, W.R., da Silva Nunes, E.; dos Santos, C.C.; William da Silva, S.; Aragon, F.H.; Huamani, Coaquirá J.A.; Cesar Morais, P.; Jafelicci, Jr M., (2013). PEGylation of SPIONs by polycondensation reactions: a new strategy to improve colloidal stability in biological media. *J. Nanopart. Res.*, 15: 1824-1835.
- Wang, Z.; Zhu, J.; Chen, Y.; Geng, K.; Qian, N.; Cheng, L.; Lu, Z.; Pan, Y.; Guo, L.; Li, Y.; Gu, H., (2014). Folic acid modified superparamagnetic iron oxide nanocomposites for targeted hepatic carcinoma MR imaging. *RSC Adv.*, 4, 7483-7490.
- Ying, T.Y.; Yiaccoumi S.; Tsouris C., (2002). An electrochemical method for the formation of magnetite particles. *J. Dispersion Sci. Technol.*, 23: 569-576.
- Yao, K.; Gong, J.; Tian, N.; Lin, Y.; Wen, X.; Jiang, Z.; Na, H.; Tang, T., (2015). Flammability properties and electromagnetic interference shielding of PVC/graphene composites containing Fe₃O₄ nanoparticles. *RSC Adv.*, 5: 31910-31919.

AUTHOR (S) BIOSKETCHES

Isa Karimzadeh, Ph.D. Candidate, Shefa Neuroscience Research Center, Khatam ol Anbia Specialty and Subspecialty Hospital, Tehran, Iran

Mustafa Aghazadeh, Assistant Professor, NFCRI, Nuclear Science and Technology Research Institute (NSTRI), P.O. Box 14395-834, Tehran, Iran, *E-mail:* maghazadeh@aeoi.org.ir

Simindokht Shirvani-Arani, Assistant Professor, NFCRI, Nuclear Research Institute, Tehran, Iran